Design and Kinematics Analysis of a Continuum Throat Surgery Robot

W L Peng[a], Y N Zhang[b], L Y Shen[c] and J W Qian[d]

School of Mechatronic Engineering and Automation, Shanghai University, 99 Shangda Road, Baoshan District, Shanghai, China

[a]pengwanglong@foxmail.com; [b]ynzhang@shu.edu.cn; [c]shenlycn@163.com; [d]jwqian@shu.edu.cn;

Abstract. A cable-driven continuum throat surgery robot is designed in this paper, which is a new type of bionic robot with softness and flexibility. Throat surgery robot in the market has the disadvantage of large-scale wound and discomfort, robot in this can solve these problem. Firstly, the joint of the robot is modularized by simulating the skeleton of the snake, and the modules are connected by spherical joints to simulate the high flexibility of the snake. Secondly, each part of the robot is controlled by three cables to control the bending motion in the pitch and yaw directions. Lastly, the kinematics analysis is carried out by the D-H method, including the mapping of the driving space, joint space and operation space of the joint module. According to the entity we make, it is approved that the robot has the advantages of small structural size, high positioning accuracy, and strong space flexibility for that the structure of the snake robot is integrated with the drive of the continuous robot. It is ideal for transoral throat surgery, and the operation is performed through the natural cavity to ensure the accuracy and safety of the operation, and the postoperative recovery is also faster.

1. Introduction

The throat is connected to the esophagus, larynx, and oropharynx. For the human body, it is an important transportation hub, and it also has many important structures and functions. Nasopharyngeal carcinoma is one of the most common malignant tumors and is harmful to human health [1]. About 80 percent of nasopharyngeal carcinomas in the world occur in China [2].

At present, throat examination and treatment are mainly assisted by self-retaining laryngoscope, while the throat is a small cavity, deep space, and is difficult to observe [3]. Therefore, the use of self-retaining laryngoscope in throat surgery will cause strong discomfort to the patient, and the patients' instinctive swallowing and other actions can also affect the doctor's operation which greatly influence the operation effect. In addition, when the surgeon is undergoing surgery, the involuntary tremor of the arm may touch the human body and may cause great damage. When it is necessary to cut directly from the outside, the wound area of the conventional throat surgery is large and the surgery is difficult to operate for that the view of the surgery is small, and postoperative infection and pharyngeal leakage can easily occur.

The continuous robot is a new bionic robot, which has good bending performance and can change its shape softly and flexibly, and its excellent bending characteristics is the same as some biological organs like snake body, octopus antenna, elephant nose and so on[4]. Due to the shape of the continuous robot can be flexibly transformed, it can change its shape according to the condition of the

environmental obstacle, and has unique adaptability to a work space-limited environment [5]. The continuum robot is applied to the medical operation, and the robot can reach the affected part by the human body natural cavity or the minimally invasive mouth, thus reducing the difficulty of the operation, avoiding the discomfort caused by the use of self-retaining laryngoscope and the disadvantages of the large-scale wound in traditional operation. It has the advantages of light pain, wound healing faster after surgery, and less tremor which ensure the accuracy and safety of surgery [6]. Therefore, the surgical robot through the natural cavity of the human body has received extensive attention in recent years and more and more scholars have studied it. Medrobotics has research on the application in the medical field of continuum robots. The company's Flex Robotic System is relatively excellent and has already been successfully commercialized [7-8].

The special needs of throat surgery are analyzed in this paper, the structure of the cable-driven throat surgery continuum robot is designed by reference to the shape of the Medrobotics' Flex robot, and its movement mode is introduced. This paper analysis the mapping connection between the task space, joint space and cable-driven space of the continuum robot, and completed the kinematic decoupling analysis of the driving space and joint space between the multi-joint modules of the cable-driven robot by D-H method. Thereby the kinematics problem of the continuum robot is solved. The correctness of the relevant kinematics algorithm is verified by the analysis of the robot workspace.

2. Demand analysis and robot design

2.1. Analysis of demand

To enable the robot to have the ability to assist throat surgery in a narrow space, the main functions requirements of the robot are as follows: (I) Sports flexibility, (II) Small size.

As shown in Figure 1(a), the snake bones are mainly divided into three types: skull, spine, and ribs. The body is long and soft, and it is composed between 100 to 400 connected bones [9]. Although the range of motion between adjacent vertebrae is small, the whole body of the snake can form a large bending angle through the combination of multiple vertebral. The surgical robot adopts the modular design of the joint to simulate the spine of the snake, and the joint modules are hinged by the spherical joints. Therefore the structure is compact and smaller. The single joint has multiple degrees of freedom and the bending performance is good, so that the robot realizes the bending motion which is similar to the biological snake, and achieves the requirement of motion flexibility. Because the cable-driven has the advantages of the fixed drive source, high positioning accuracy, and lightweight, the robot uses the cable-driven to realize the remote control capability. The robot designed in this paper reserves the sensor channel inside, which can integrate multiple sensors such as light source and camera to improve the perception of the doctor of the narrow space, realize the exploration of the unknown space and complete the motion planning.

The structure parameters of the continuous robot are calculated independently. The robot is two concentric mechanisms, one is the outer link and the other is the inner link. They all follow the modular design of the joint and use the joint module to imitate the spine of the snake as shown in Figure 1 (b), and the two adjacent links cooperate to form a spherical joint articulation. The laryngoscope surgery space is about an elliptical column with long diameter of 20 mm, short diameter of 35mm and height of 175mm, and the laryngoscope surgery space is similar to the throat space [10], therefore the outer link has an outer diameter of 17mm and the maximum bending angle between the joints is degree of 13.
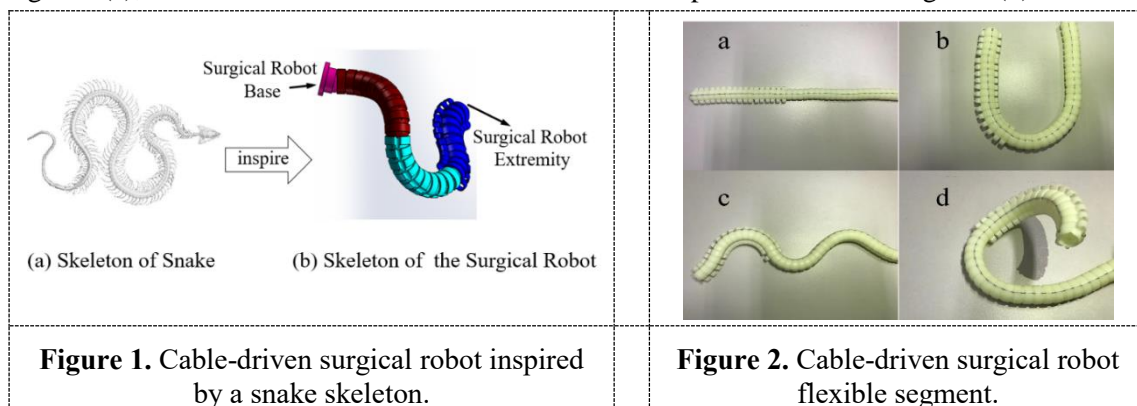
The main function of the outer link is to act as the main support for the skeleton and guide the robot to drive the cable. The diameter of the cable guide hole is 0.9mm, which is evenly distributed on the 15.5mm circle. The outer link module has 35 knots, and the total length is 264mm. The main function of the inner link is to realize the feed motion of the robot with the outer link and realize the component passage with the outer link. The center cable guide hole is 2.2mm, the inner link module has 48 knots, and the total length is 270mm. The specific module parameters are shown in Table 1. After the outer link and the inner link is assembled, the groove on the link can form three diameter of 2mm passages

which are made for passing the elongate members such as cables, sensors, and surgical tools.
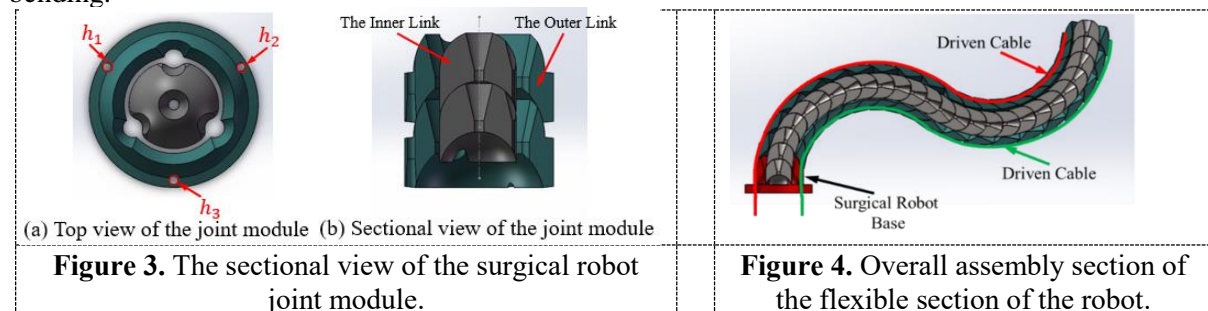
Table 1. Parameters of joint module.

Parameters	Outer Diameter (mm)	Inner Diameter (mm)	Spherical Diameter (mm)	Pilot Hole Reference Circle Diameter (mm)	Groove Reference Circle Diameter (mm	Node Height (mm)	Gap distance (mm)
Outer Links	17	10	15	0.9	15.5	9.5	5.8
Inner Links	9	2.2	9			9.5	0.796

The internal and external mechanisms have been physically produced by combining SolidWorks and 3D printing techniques. The robot is in the vertical direction as shown in Figure 2(a), and the robot bends once in the plane as shown in Figure 2(b). The robot bends in the plane as many times as shown in Figure 2(c), and the robot bends in the three-dimensional space as shown in Figure 2(b).

Figure 1. Cable-driven surgical robot inspired by a snake skeleton.

Figure 2. Cable-driven surgical robot flexible segment.

For a single joint module, it has two degrees of freedom of pitch and yaw, and the cable can transmit tension but can't withstand pressure, thus the joint module has at least 3 drive cables for free movement [11]. In addition, the structure of the robot should be as small as possible. Therefore, the outer link uses three drive cables, and the angle between the two adjacent cables is degree of 120. The cable in the center of the inner link controls the switching between the flexibility and the rigid state of the internal mechanism as shown in Figure 3. Through this driving method, the robot can realize three-dimensional space motion, feed motion, and can go forward in the tortuous channel.

Figure 4 is a cross-sectional view of the flexible section of the robot. The whole flexible section is hinged of spherical joints, the cable passing through the guide hole and fixed at the distal end of the robot. The slight angle between the spherical joints is changed through the extension or contraction of the three cables, and the single bending motion of the laryngeal surgery robot is completed by accumulating the slight relative motion which is between the spherical joints. The multiple bending motion of the robot is completed by the cooperation of the internal mechanism and the external mechanism, which can achieve the forward movement in a torturous environment. Besides, when the length of the cable changes, the load on the robot can be transformed to the axial force and torque for that the nodes are rigid. The axial strain is negligible, as a result the movement of the robot is pure bending.


Figure 3. The sectional view of the surgical robot joint module.

Figure 4. Overall assembly section of the flexible section of the robot.

2.2. Feed movement and squat movement

In this paper, both internal and external mechanisms are structures that can be manipulated independently. The internal mechanism is called the inner core mechanism. The external mechanism is called the outer casing mechanism. Each mechanism can be switched between a flexible state and a rigid state, therefore it can be shaped according to the complex environment by the repeated switch of different states. The flexible state does not mean that the structure of the robot passively depends on gravity or its environment. It is not slack and passive but articulated and controllable to reach a given location.

The state between the two mechanisms can be alternately switched. When one mechanism is in rigid state, the other will be in flexible state. For illustration purposes, it is assumed that the outer casing mechanism is in rigid state at the initial stage and the inner core mechanism is in flexible state as shown in step 1 in Figure 5, and the mechanisms are pushed forward by the feed mechanism.

The feeding mechanism pushes the outer casing mechanism forward, and the turning direction of the outer casing mechanism is controlled by the variation of cable length. At this moment, the outer casing mechanism is in flexible state, and the rope of the inner core mechanism is tightened to make the inner core mechanism is in rigid state. The path that the robot has passed before is remembered by the inner core mechanism as shown step 2 in Figure 5. Then the rope of the outer casing mechanism is tightened and the rope of the inner core mechanism is relaxed to switch the state of the internal and external mechanisms. The outer casing mechanism is in rigid state, and the inner core mechanism is in flexible state. After the states are alternated, the inner core mechanism is pushed forward to coextend with the outer casing mechanism as shown step 3 in Figure 5. By repeating the above process, the bending movement of the robot can be achieved, to reach the desired location, such as the throat of human.

Figure 5. Schematic diagram of robot feed motion and bending motion.
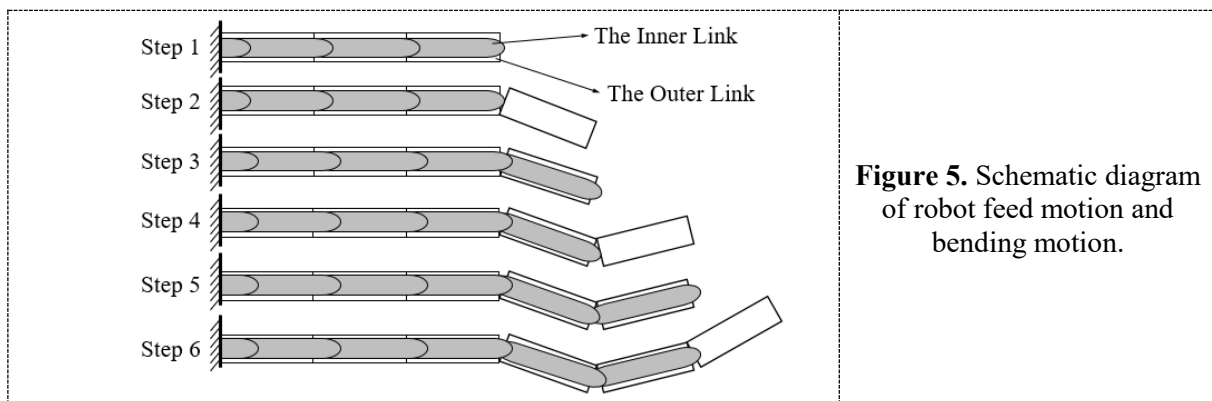
In practical applications of transoral throat surgery, once the continuum robot reach the desired position, the affected part. The operator can remove the inner core mechanism and insert the surgical tool along the outer casing mechanism to operation.

3. Kinematics formula and modeling

Based on the structural design, this paper further makes the kinematics analysis and modeling, the D-H parameter method is used in this paper [12]. Since the number of joints of the robot is relatively large and the kinematics analysis is relatively complicated, in addition to the mapping relationship between the joint space and the task space in the conventional robot, it is also necessary to consider the complex mapping relationship between the joint space and the cable-driven space. Therefore, its kinematic spatial mapping relationship is shown in Figure 6.

According to Figure 6, the kinematics analysis of the robot is completed by two steps:

(I) Solving the relationship of forward and inverse kinematics between task space and joint space, and obtaining the formula between position, posture of the distal end of the robot in three-dimensional space and θ, Φ of the joint module.

(II) Solving the relationship of forward and inverse kinematics between cable-driven space and joint space, and obtaining the formula between θ, Φ of the joint module and the cable length variation Δli.
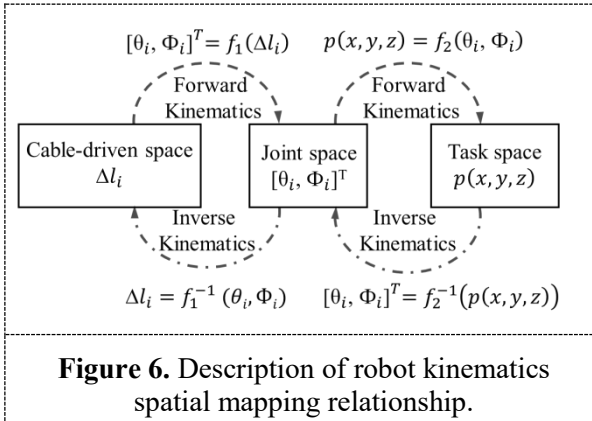
Figure 6. Description of robot kinematics spatial mapping relationship.
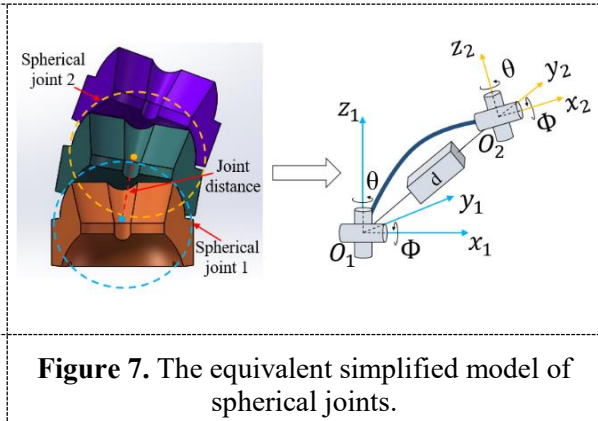
Figure 7. The equivalent simplified model of spherical joints.

### 3.1. Forward kinematics between task space and joint space

For the continuous flexible section of the robot, the spherical joint can be described as three rotating joints and a zero length link [13]. However, the cable for the transmission constrains the rotational motion around its own axis, the spherical joint is simplified into two rotating joints and a fixed-length connecting link d which represents the joint distance between the two adjacent spherical joints. The spherical joint equivalent simplified model is shown in Figure 7.

Due to the extreme bending angle of the 15 external link modules is degree of 182, the robot can meet the most of bending requirements. In the equivalent model, the homogeneous coordinate transformation matrix of the end reference to the fixed coordinate system and the D-H parameter table can be calculated by establishing the corresponding coordinate system on the 15 joints. The D-H coordinate system is shown in Figure 8.

According to the D-H parameter table established principles, the D-H parameters corresponding to the 15 joints of the flexible section are obtained in turn as shown in Table 2.

Table 2. D-H Parameters.

Link i	1	2	3	4	5	6	……	25	26	27	28
$a_i(mm)$	0	0	h_0	0	h_0	0	……	h_0	0	h_0	0
$\alpha_i(°)$	0	90	-90	90	-90	90	……	-90	90	-90	90
$d_i(mm)$	0	0	0	0	0	0	……	0	0	0	0
$\theta_i(°)$	θ_1	θ_2	θ_1	θ_2	θ_1	θ_2	……	θ_1	θ_2	θ_1	θ_2
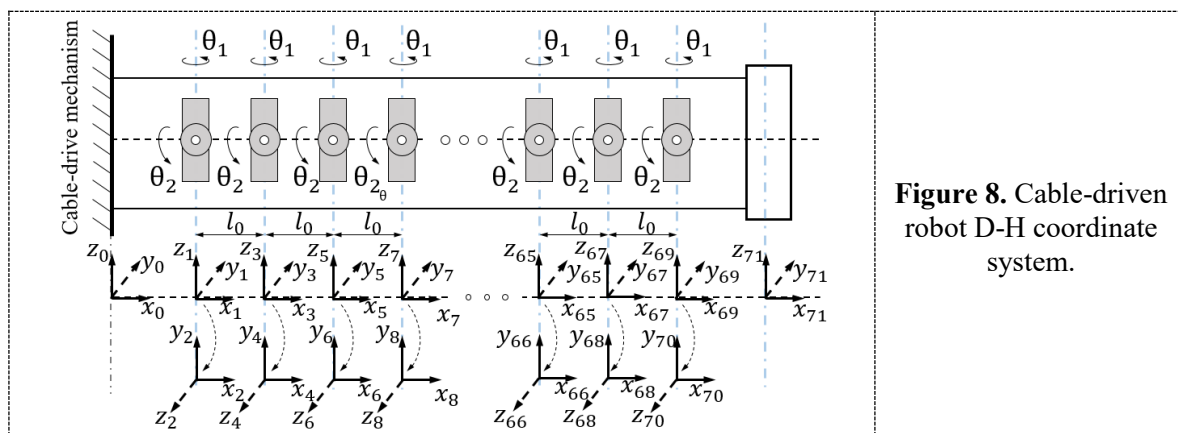
Figure 8. Cable-driven robot D-H coordinate system.

Then based on the D-H parameter table and the principles of homogeneous transformation matrix, all the homogeneous transformation matrices of joints are obtained in order as follows:

$$
{}^0_1T = \begin{pmatrix} c_{\theta_1} & -s_{\theta_1} & 0 & 0 \\ s_{\theta_1} & c_{\theta_1} & 0 & 0 \\ 0 & 0 & 1 & 0 \\ 0 & 0 & 0 & 1 \end{pmatrix} \tag{1}
$$

$$
{}^1_2T = \begin{pmatrix} c_{\theta_2} & -s_{\theta_2} & 0 & 0 \\ 0 & 0 & -1 & 0 \\ s_{\theta_2} & c_{\theta_2} & 0 & 0 \\ 0 & 0 & 0 & 1 \end{pmatrix} \tag{2} \quad
{}^2_3T = \begin{pmatrix} c_{\theta_1} & -s_{\theta_1} & 0 & h_0 c_{\theta_1}(1 - c_{\theta_1})/\theta_1 \\ 0 & 0 & 1 & h_0 s_{\theta_2}(1 - c_{\theta_1})/\theta_1 \\ -s_{\theta_1} & -c_{\theta_1} & 0 & h_0 s_{\theta_1}/\theta_1 \\ 0 & 0 & 0 & 1 \end{pmatrix} \tag{3}
$$

$$
{}^3_4T = \begin{pmatrix} c_{\theta_2} & -s_{\theta_2} & 0 & 0 \\ 0 & 0 & -1 & 0 \\ s_{\theta_2} & c_{\theta_2} & 0 & 0 \\ 0 & 0 & 0 & 1 \end{pmatrix} \tag{4} \quad
{}^4_5T = \begin{pmatrix} c_{\theta_1} & -s_{\theta_1} & 0 & h_0 c_{\theta_1}(1 - c_{\theta_1})/\theta_1 \\ 0 & 0 & 1 & h_0 s_{\theta_2}(1 - c_{\theta_1})/\theta_1 \\ -s_{\theta_1} & -c_{\theta_1} & 0 & h_0 s_{\theta_1}/\theta_1 \\ 0 & 0 & 0 & 1 \end{pmatrix} \tag{5}
$$

In the single bending motion, the representation of the end coordinate system in the reference coordinate system can be calculated by multiplying the homogeneous transformation matrices calculated above in turn, which is the forward kinematics solution of the robot in the single bending motion:

$$
{}^0_{28}T = {}^0_1T \cdot {}^1_2T \cdot {}^2_3T \cdots {}^{26}_{27}T \cdot {}^{27}_{28}T = f(\theta_1, \theta_2) \tag{6}
$$

3.2. Inverse kinematics between task space and joint space

The trajectory planning of the robot depends on the inverse kinematics solution between the task space and the joint space [14], and the trajectory planning has an influence on the motion control and the completion of the task, therefore the inverse kinematics is an important factor affecting the control precision and response precision of the robot. The inverse kinematics solution between the task space and joint space which can calculate the angular variables between the joint modules of the robot is according to the position, posture of the end of the robot. Since the joints of the cable-driven robot are special, the inverse of their kinematics is not unique.

The specific inverse kinematics solution process can be described as: according to the desired pose X of the end of the robot in the task space, the pose difference dX between the current pose and the desired pose can be obtained. The Jacobian matrix J is calculated by equation (5), thus the relationship between dX and the joint variable d_θ can be acquired. Using $(\theta + d_\theta)$ as a new input to the robot joint, the motion of the robot can be controlled to realize the motion of the robot as followed:

$$
\text{dX} = J(\theta)d_\theta \tag{7}
$$

$$
J^+ = J^T(JJ^T)^{-1} \tag{8}
$$

Where J is the Jacobian matrix of the robot in the current state, and J+ is the generalized inverse matrix corresponding to J.

Therefore the inverse kinematics solution of the robot is:

$$
d_\theta = J^+ \text{dX} \tag{9}
$$

3.3. Forward kinematics between cable-driven space and joint space

The throat surgery robot has three cable inputs and two degrees of freedom motion output for three-dimensional motion. The length of cables inside the joint modules are fixed, and the angle variation between joint modules is caused by the length of cables variation which are between the joint modules. This paper has established a simplified kinematic model of the joint module to describe the relationship between the cable-driven space and the joint space as shown in Figure 9. The plane $B_1B_2B_3$

and $A_1A_2A_3$ respectively represent the upper end planes of the joint module 1 and the joint module 2. The line segments A_1B_1, A_2B_2, and A_3B_3 respectively represent three driving cables l_1, l_2, and l_3. The center O_1 of the plane $B_1B_2B_3$ and the center O_2 of the plane $A_1A_2A_3$ are taken as the origin, the direction of the axis which belongs to the joint module is taken as the Z-axis, and the direction of two rotation for joint are taken as the X and Y axes to respectively establish coordinate systems {1} and {2}.
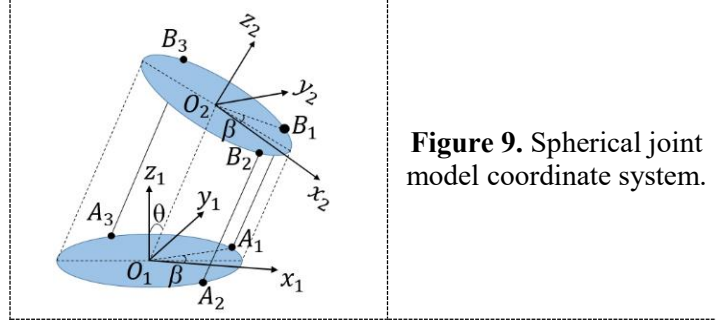
Figure 9. Spherical joint model coordinate system.

Assuming that initial distance between the two origin of the joint module is h0. For the coordinate system {1} and {2}, {1} rotates θ degree around its X-axis, rotates ψ degree around its Y-axis, and continue to translate h0 along the Z-axis which has already been rotated, and as a result {1} will coincide with {2}. The homogeneous transformation matrix between {1} and {2} as follows:

$$\tfrac{1}{2}T = Rot(X,\ \theta)ROT(Y,\psi)Trans(0,0,h_0) \tag{10}$$

$$= \begin{bmatrix} c_\psi & 0 & s_\psi & 0 \\ s_\theta s_\psi & c_\theta & -s_\theta c_\psi & 0 \\ -c_\theta s_\psi & s_\theta & c_\theta c_\psi & 0 \\ 0 & 0 & 0 & 1 \end{bmatrix} \begin{bmatrix} 1 & 0 & 0 & 0 \\ 0 & 1 & 0 & 0 \\ 0 & 0 & 1 & h_0 \\ 0 & 0 & 0 & 1 \end{bmatrix} = \begin{bmatrix} c_\psi & 0 & s_\psi & s_\psi h_0 \\ s_\theta s_\psi & c_\theta & -s_\theta c_\psi & -s_\theta c_\psi h_0 \\ -c_\theta s_\psi & s_\theta & c_\theta c_\psi & c_\theta c_\psi h_0 \\ 0 & 0 & 0 & 1 \end{bmatrix}$$

Take point A_1 arbitrarily on the upper-end plane of the joint module 1. $\angle A_1O_1X_1$ is equal to β in Figure 8, then the point B_1 corresponding to A_1 on the upper-end plane of the joint module 2 is also $\angle B_1O_2X_2$ is equal to β, therefore in the {1} coordinate system:

$$\begin{cases} {}^1A_1 = [rc_\beta \quad rs_\beta \quad 0 \quad 1]^T \\ {}^2B_1 = [rc_\beta \quad rs_\beta \quad 0 \quad 1]^T \end{cases} \tag{11}$$

By homogeneous transformation, 1B1 in the {1} coordinate system can be calculated as follows:

$$^1B_1 = {}^1T_2\,{}^2B_1 = \begin{bmatrix} rc_\psi c_\beta + s_\psi h_0 \\ rs_\theta s_\psi s_\beta + rc_\theta s_\beta h_0 - s_\theta c_\beta h_0 \\ -rc_\theta s_\psi c_\beta + rs_\theta s_\beta h_0 + c_\theta c_\beta h_0 \\ 1 \end{bmatrix} \tag{12}$$

The length l1 of the cable A_1B_1 can be calculated as follows:

$$|A_1B_1| = \left[\left(rc_\psi c_\beta + s_\psi h_0 - rc_\beta\right)^2 + \left(rs_\theta s_\psi s_\beta + rc_\theta s_\beta h_0 - s_\theta c_\beta h_0 - rs_\beta\right)^2 \right.$$

$$\left. + \left(-rc_\theta s_\psi c_\beta + rs_\theta s_\beta h_0 + c_\theta c_\beta h_0\right)^2 \right]^{\tfrac{1}{2}} \tag{13}$$

Similarly, for the cables A_2B_2 and A_3B_3 there are:

$$|A_2B_2| = \left[\left(rc_\psi c_{\beta+\frac{2}{3}\pi} + s_\psi h_0 - rc_{\beta+\frac{2}{3}\pi}\right)^2 + \left(rs_\theta s_\psi s_{\beta+\frac{2}{3}\pi} + rc_\theta s_{\beta+\frac{2}{3}\pi} h_0 - s_\theta c_{\beta+\frac{2}{3}\pi} h_0 - rs_{\beta+\frac{2}{3}\pi}\right)^2 \right.$$

$$\left. + \left(-rc_\theta s_\psi c_{\beta+\frac{2}{3}\pi} + rs_\theta s_{\beta+\frac{2}{3}\pi} h_0 + c_\theta c_{\beta+\frac{2}{3}\pi} h_0\right)^2 \right]^{\tfrac{1}{2}} \tag{14}$$

$$|A_3B_3| = \left[\left(rc_\psi c_{\beta+\frac{4}{3}\pi} + s_\psi h_0 - rc_{\beta+\frac{4}{3}\pi}\right)^2 + \left(rs_\theta s_\psi s_{\beta+\frac{4}{3}\pi} + rc_\theta s_{\beta+\frac{4}{3}\pi} h_0 - s_\theta c_{\beta+\frac{4}{3}\pi} h_0 - rs_{\beta+\frac{4}{3}\pi}\right)^2 \right.$$

$$+ \left(-rc_\theta s_\psi c_{\beta+\frac{4}{3}\pi} + rs_\theta s_{\beta+\frac{4}{3}\pi} h_0 + c_\theta c_{\beta+\frac{4}{3}\pi} h_0 \right)^2 \Big]^{\frac{1}{2}} \tag{15}$$

Where s is short for the sine function, c is short for the cosine function, $\theta \in [0, \pi]$, $\psi \in [0, \pi]$, h_0 is one unit length of the outer link of the continuum robot.

3.4. Inverse kinematics between cable-driven space and joint space

The plurality of joint modules of the cable-driven robot can be regarded as series structure, therefore when the robot moves, the motion of the joint module near the base portion will coupled with all the subsequent joint motion modules which are close to the end. The kinematic decoupling analysis between the cable-driven space and joint space is to eliminate the coupling effect of the front joint modules step by step, and the amount of variation in the length of each cable are calculated one by one as an inverse kinematic solution.

Due to the first joint module is not coupled to any other joint modules, the cable length variation of the nth ($1 < n \leq 28$) decouped joint modules is Δli (i = 1, 2, 3), and the angular variable of the joint is θ_n, ψ_n. This paper assumes that the position of the first driving cable on the upper end plane of the joint module is βn, therefore the variation of the three cables as follows:

$$\Delta l_{n1} = f(\theta_n, \psi_n, \beta_n) + f(\theta_{n-1}, \psi_{n-1}, \beta_n) + \cdots + f(\theta_1, \psi_1, \beta_n) - nd \tag{16}$$

$$\Delta l_{n2} = f\left(\theta_n, \psi_n, \beta_{n+\frac{2}{3}\pi}\right) + f\left(\theta_{n-1}, \psi_{n-1}, \beta_{n+\frac{2}{3}\pi}\right) + \cdots + f\left(\theta_1, \psi_1, \beta_{n+\frac{2}{3}\pi}\right) - nd \tag{17}$$

$$\Delta l_{n3} = f\left(\theta_n, \psi_n, \beta_{n+\frac{4}{3}\pi}\right) + f\left(\theta_{n-1}, \psi_{n-1}, \beta_{n+\frac{4}{3}\pi}\right) + \cdots + f\left(\theta_1, \psi_1, \beta_{n+\frac{4}{3}\pi}\right) - nd \tag{18}$$

Where $f(\theta, \psi, \beta)$ represents the formula for calculating the length of each of the three cables.

3.5. Simulation and analysis of the workspace

The workspace of the robot mainly depends on its structure, which is the maximum bending angle between each joint module and the number of modules. Due to the joint bending angle and the distance between the joints, the workspace is only a part of the spherical surface. The spherical radius depends on the bending angle of the joint and the distance between the joints.

The workspace of the multi-joint module is more complicated. Based on the design parameters and kinematics analysis of the robot in the previous statement, the workspace is simulated with the Monte Carlo method which based on random probability by the MATLAB Robotics Toolbox in this paper [15]. A random value that produces 30,000 joint variables is substituted into the position vector of the kinematic equation to obtain a cloud map composed of random points, which constitutes the Monte Carlo workspace of the robot as shown in Figure 10.
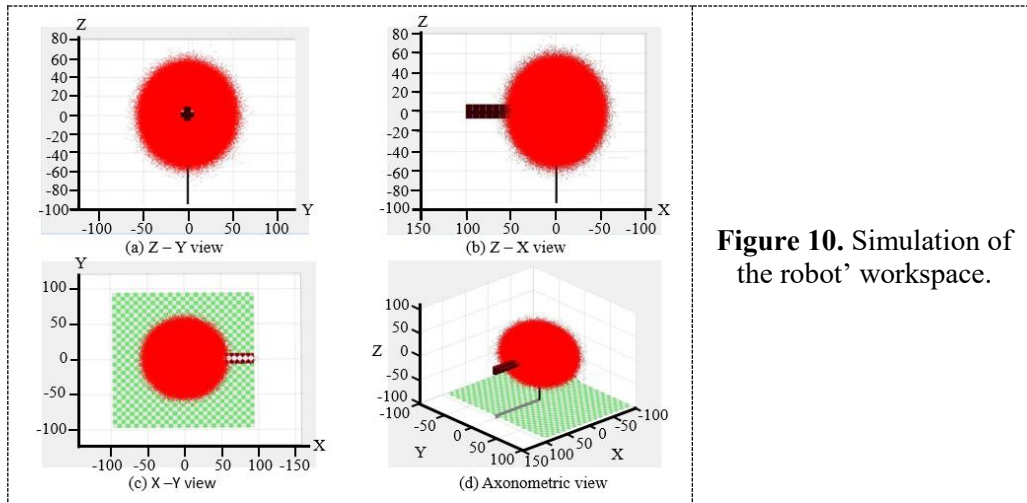
Figure 10. Simulation of the robot' workspace.

The workspace of the robot is a sphere space, and the longest distance that can be reached is 60mm. The workspace is a sphere space with a radius of 60mm without singular point, therefore it can reach any position in the sphere. Therefore, the cable-driven robot which is series connected of joint modules has a large working space in three-dimensional space, and the flexible movement of the robot in three-dimensional space can be realized. From the simulation results, the workspace of the robot can be directly observed, which verifies the correctness of the relevant kinematics algorithms, and lays a good foundation for further study of the trajectory planning and control of the modular robot.

4. Conclusions

This paper designs the structure of a cable-driven continuum surgical robot. The snake-shaped robot and the continuum robot are combined to make the robot has the advantages of high precision and small structure. The demand analysis and design of the cable-driven robot are described. In addition, the forward and inverse kinematics of the robot are discussed and explained, and the workspace of the robot is analyzed. Due to its compact construction and high flexibility, the robot is able to achieve the flexibility required for surgery without having to touch tissue outside the affected area. It enters the human body through the natural cavity of the human body, which ensures the accuracy and safety of the operation. The innovation of this research is to refer to the shape of the Flex robot of Medrobotics. The structure parameters of the robot are given by calculation and verification, and the forward and inverse kinematics analysis and kinematic decoupling are performed by DH parameter method to solve the complex motion space mapping problem of continuum robot. The relevant kinematics algorithm is verified by the analysis of the robot workspace. However, the control part of this article has not been perfected and needs further research in the future.

References

[1]   Yan S Q, Wang J Z, and Yu S 2018 Advance in design and application of self-retaining laryngoscope *International Journal of Otorhinolaryngo-logy Head and Neck Surgery* (vol 42) chapter 5 pp 302-6

[2]   Roy S and Smith B 2016 Robtic surgery in pediatric otolaryngology *Int J Head Neck Surg* (vol 7) chapter 2, pp 120-3

[3]   Friedrich D T, Dürselen L, and Mayer B 2017 Features of haptic and tactile feedback in TORS-a comparison of available surgical systems *Journal of Robotic Surgery* (vol 12) chapter 10 pp 1-6

[4]   Xu K 2009 Design, modeling and analysis of continuum robots as surgical assistants with intrinsic sensory capabilities *Dissertations & Theses - Gradworks* pp 467-72

[5]   Wei W, Xu K, and Simaan N 2006 A compact two-armed slave manipulator for minimally invasive surgery of the throat *IEEE Annel. Biomedical Robotics and Biomechatronics* (vol 2) pp 740-1 200-6

[6]   Zheng L, Liang R H, and Philip W Y C 2016 A novel constrained wire-driven flexible mechanism and its kinematic analysis *Mechanism and Machine Theory* (vol 95) pp 59-75

[7]   Ian J D, Arnold E O, and Joseph A S 2015 Introduction devices for highly articulated robotic probes and methods of production and use of such probes U.S 0005683

[8]   Mandapathil M, Greene B, and Wihelm T 2015 Transoral surgery using a novel single-port flexible endoscope system *European Archives of Oto-rhino-Laryngology* (vol 272) chapter 9 pp 2451-56

[9]   Dong X, Raffles M, and Guzman S C 2014 Design and analysis of a family of snake arm robots connected by compliant joints *Mechanism and Machine Theory* (vol 77) pp 73-91

[10]   Tonapi M M, Godage I S, and Vijaykumar A M 2015 A novel continuum robotic cable aimed at applications in space *Advanced Robotics* (vol 29) chapter 13 pp 861-75

[11]   Hirose S and Mori M August 2004 Shenyang China Biologically inspired snake like robots *IEEE International Conference on Robotics and Biomimetics* (vol 2) pp 22-26

[12]   Carricato M and Merle J P 2013 Stability analysis of underconstrained cable-driven parallel

robots *IEEE Transactions on Robotics (*vol 29*)* chapter 1 pp 288-96

[13] Runtian Y U, Fang Y, and Guo S 2015 Design and kinematic performance analysis of a cable-driven parallel mechanism for ankle rehabilitation *Robot (*vol 37*)* chapter 1 pp 53-62

[14] Ng A T, Tam P C 2014 Current status of robot-assisted surgery *Hong Kong medical journal (*vol 20*)* chapter 3 pp 241-50

[15] Simaan N, Xu K, and Wei W 2009 Design and integration of a telerobotic system for minimally invasive surgery of the throat *The International Journal of Robotics Research (vol 28)* chapter 9 pp 1134-53